Catalytic Behavior of K-doped Fe/MgO Catalysts for Ammonia Synthesis Under Mild Reaction Conditions

Kohei Era,[a] Katsutoshi Sato,*[a,b] Shin-ichiro Miyahara,[a] Takahiro Naito,[c] Kanishka De Silva,[c] Saeid Akrami,[c] Hiroshi Yamada,[a] Takaaki Toriyama,[d] Tomokazu Yamamoto,[d] Yasukazu Murakami,[d,e] Ken-ichi Aika,[f] Koji Inazu,[f] and Katsutoshi Nagaoka*[a,c]

[a] K. Era, Dr. K. Sato,* S. Miyahara, Dr. H. Yamada, Prof. Dr. K. Nagaoka*
Department of Chemical Systems Engineering, Graduate school of Engineering
Nagoya University
Furo-cho, Chikusa-ku, Nagoya, 464-8603, Japan
E-mail: sato.katsutoshi@marerial.nagoya-u.ac.jp, nagaoka.katsutoshi@material.nagoya-u.ac.jp

[b] Dr. K. Sato
Institute for Advanced Research
Nagoya University
Furo-cho, Chikusa-ku, Nagoya, 464-8603, Japan

[c] Dr. T. Naito, Dr. K. De Silva, Dr. S. Akrami, Prof. Dr. K. Nagaoka
Institutes of Innovation for Future Society
Nagoya University.
Furo-cho, Chikusa-ku, Nagoya, 464-8603, Japan

[d] T. Toriyama, Dr. T. Yamamoto, Prof. Dr. Y. Murakami
The Ultramicroscopy Research Center
Kyushu University
Motooka 744, Nishi-ku, Fukuoka, 819- 0395, Japan

[e] Prof. Dr. Y. Murakami
Department of Applied Quantum Physics and Nuclear Engineering,
Kyushu University
Motooka 744, Nishi-ku, Fukuoka, 819-0395, Japan

[f] Prof. Dr. K. Aika, Prof. Dr. K. Inazu
National Institute of Technology, Numazu College
3600 Ooka, Numazu, Shizuoka, 410-8501, Japan

Supporting information for this article is given via a link at the end of the document.

Abstract: An important part of realizing a carbon-neutral society using ammonia will be the development of an inexpensive yet efficient catalyst for ammonia synthesis under mild reaction conditions (<400 °C, <10 MPa). Here, we report Fe/K(3)/MgO, fabricated *via* an impregnation method, as a highly active catalyst for ammonia synthesis under mild reaction conditions (350 °C, 1.0 MPa). At the mentioned conditions, the activity of Fe/K(3)/MgO (17.5 mmol h^{-1} g_{cat}^{-1}) was greater than that of a commercial fused iron catalyst (8.6 mmol h^{-1} g_{cat}^{-1}) currently used in the Haber–Bosch process. K doping was found to increase the dispersion and turnover frequency of Fe in our Fe/K(3)/MgO catalyst. In addition, increasing the pressure to 3.0 MPa at the same temperature led to a significant improvement of the ammonia synthesis rate to 29.6 mmol h^{-1} g_{cat}^{-1}, which was much higher than that of two more expensive, benchmark Ru-based catalysts, which are also potential alternative catalysts. A kinetics analysis revealed that the addition of K dramatically enhanced the ammonia synthesis activity at ≥300 °C by changing the main adsorbed species from NH to N which can significantly accelerate dissociative adsorption of nitrogen as the rate limiting step in ammonia synthesis.

Introduction

Ammonia (NH_3) is one of the most important chemical feedstocks in modern society. Currently, global NH_3 production is about 200 million tons per year, and more than 80% of this amount is used as fertilizer for the production of food for almost half the world's population. [1] Due to universal concerns regarding global warming caused by the emission of CO_2, NH_3 has attracted attention for its potential as a carrier of hydrogen for use as a renewable energy and decarbonized fuel. However, there are many challenges that must be overcome to realize widespread utilization of NH_3 as part of a carbon-neutral energy society. [1b, 2]

Most ammonia is synthesized by the reaction of nitrogen and hydrogen through what is known as the Haber–Bosch (HB) process. Although this process is very well-optimized, the hydrogen used in this reaction comes from the reforming of fossil fuels, which results in high global emission of CO_2 (1.9 tons NH_3^{-1}). [3] Thus, because NH_3 production has a marked impact on global warming, decarbonization of the HB process will be a necessary step toward achieving a sustainable future society.

In the conventional commercial HB process, a fused Fe-based catalyst has been used since its discovery by Mittasch. [4] This catalyst is doped with Al_2O_3 (structural promoter) and K_2O (chemical promoter) to accelerate N_2 triple bond cleavage (bond dissociation energy, 945 kJ mol^{-1}), which is the rate-determining

step for NH_3 synthesis. However, this catalyst is not suitable for a green NH_3 synthesis process because it requires a high temperature and pressure (>450 °C, >20 MPa). [4] Therefore, to efficiently synthesize green NH_3 using hydrogen derived from renewable energy sources, it will be crucial to reduce the temperature and pressure of the NH_3 synthesis process by developing catalysts that are sufficiently active under mild reaction conditions (<400 °C, <10 MPa). [5]

Ru-based catalysts show high activity for NH_3 synthesis under mild reaction conditions and are regarded as potential alternatives to fused Fe-based catalysts for the HB process. However, Ru is a rare and expensive element, so it's commercial application as a catalyst for the synthesis of green NH_3 has been limited. [6] Instead, catalysts containing more abundant transition elements, namely Mn [7], Fe [8], and Co [9], have been proposed for green NH_3 synthesis. Of the proposed elements, Fe is the most abundant and economically feasible, indicating the scientific requirements to develop and promotion of Fe-based catalysts for NH_3 synthesis. While commercial fused iron catalyst does not show sufficient activity for NH_3 synthesis under mild reaction conditions, we have thought that the activity under mild reaction conditions can be improved by increasing the number of active sites, *i. e.* nanoparticulation of Fe. Several strategies have been reported to increase the number of active sites including Fe nanoparticles loading on support materials which result in enhancement of NH_3 synthesis rate. Fan *et al.* have developed a catalyst comprising FeOOH nanosheets supported on γ-Al_2O_3 and reported that the NH_3 synthesis activity of the catalyst was closely related to the Fe^0 particle size. [10] However, their developed catalyst, FeOOH-K/Al_2O_3, had poor NH_3 synthesis activity under mild conditions. Al Maksoud *et al.* and Yan *et al.* have both reported active Fe nanoparticles trapped in porous carbon nanostructures including K homogeneously prepared by solid-state pyrolysis of organometallic compounds (Metal Organic Frameworks (MOF) or phthalocyanine) and suppression of carbon removal via the methanation reaction by doping with an alkaline metal (K). [8, 11] However, utilizing a carbon material as the carrier is a concern. In all of these strategies, K is proven to enhance the rate of NH_3 synthesis, but its catalytic behavior and kinetics have not been studied well at low temperatures (<400 °C). Hattori *et al.* have demonstrated that metallic iron particles can catalyze NH_3 synthesis from nitrogen and hydrogen at 100 °C in combination with BaH_2; [12] however, their approach to catalyst preparation requires a glove box, making large-scale production impossible.

Here, we investigated the catalytic behavior and kinetics of Fe nanoparticles loaded on K-doped MgO under mild reaction conditions. We used a MgO support because we have previously reported that MgO is an effective support for Co-based catalysts that include a Co core and BaO shell and that can be prepared without the use of a glove box. [9] In the present study, we found that Fe/K(3)/MgO (K/(K + Mg) = 0.03 mol/mol) pre-reduced at 500 °C exhibited high NH_3 synthesis activity (17.5 mmol h^{-1} g_{cat}^{-1}) at 350 °C and 1.0 MPa. This value is 2.0 and 9.1 times higher than that of current commercial fused Fe catalysts per catalyst weight and Fe mass, respectively. In addition, the NH_3 synthesis rate of Fe/K(3)/MgO at 3.0 MPa was much higher than that of the benchmark Ru catalysts Ru/CeO_2 [13] and Cs^+/Ru/MgO [14]. A kinetics analysis demonstrated that the Fe catalyst was free from hydrogen poisoning, which is a typical drawback of Ru catalysts, and that its activity improved drastically with increasing pressure. We found that K doping increased the dispersion and turnover frequency of Fe in the catalyst. Furthermore, we found that the K doping dramatically increased NH_3 synthesis activity at 300 °C, not only because of electron-donating [15] to Fe^0 and/or structural modification of the active sites [10, 16], but also because of replacing main adsorbed species from NH to N.

Experimental Section

Catalyst Preparation

K-doped MgO-supported Fe catalyst (Fe/K/MgO) was prepared by sequential impregnation following our previously reported procedure. [9] First, granules of KOH (Fujifilm Wako Pure Chemicals Co., Japan) were added to ultrapure water. Then, a commercial MgO support (MgO-500A, Ube Material Industries, Ltd., Japan) was added to the aqueous solution and stirred for 1 h before removing the aqueous solvent by rotary evaporation. Hereafter, K-doped MgO support containing X mol% of K (K/(K + Mg) = X/100 mol/mol) is denoted as K(X)/MgO. The resulting powder was calcined at 500 °C for 5 h in static air. Next, the support was impregnated with iron (III) acetylacetonate [$Fe(acac)_3$] (Tokyo Chemical Industry Co., Ltd., Japan) in tetrahydrofuran (Fujifilm Wako, Japan); the Fe loading was fixed at 20 wt%. The suspension was dried using a rotary evaporator, and the resulting powder was heated at 500 °C for 5 h under an Ar stream to remove the ligand from $Fe(acac)_3$. Fe/MgO without K was prepared in the same way, except without the KOH impregnation and drying steps, and the MgO support was calcined at 500 °C for 5 h in static air before $Fe(acac)_3$ impregnation. Two benchmark Ru catalysts (Ru/CeO_2 and Cs^+/Ru/MgO) were also prepared by following our previously reported procedures. [9]

Evaluation of Ammonia Synthesis Activity

NH_3 synthesis activity was evaluated in accordance with our previous report. [9] Catalyst (100 mg) in pellet form (250–500 μm) was placed in a tubular Inconel reactor (The Nilaco Corporation, Japan) in a conventional flow system. For catalyst reduction, the temperature of the catalyst bed was raised to 500 °C at 2 °C min^{-1} under a gas stream of hydrogen–nitrogen mixture (H_2/N_2 = 3, total 240 mL min^{-1}, 0.1 MPa) and then held for 12 h. The reactor was then cooled to 200 °C in the same gas stream, a H_2-N_2 mixture with the space velocity adjusted to 72,000 mL h^{-1} g_{cat}^{-1} (H_2/N_2 = 3, total 120 mL min^{-1}) was supplied to the reactor, and the pressure was increased to 1.0 or 3.0 MPa. The NH_3 produced was trapped in an aqueous H_2SO_4 solution (1−10 mM), and the NH_3 synthesis rate was determined from the reducing rate of electronic conductivity, which was monitored with an electronic conductivity detector (CM-30R, DKK-TOA, Japan). All gases used were of high research grade (>99.9999 %), were supplied from high-pressure cylinders, and were purified using a gas purifier (MicroTorr MC50-904FV, SAES Pure Gas, USA).

Kinetic Analysis

A reaction kinetics analysis was performed at 300 or 350 °C and 0.1 MPa in accordance with previous reports. [17] Assuming that it could be described by Eq. 1, reaction rate (r) was determined by measuring the N_2, H_2, and NH_3 pressure dependences of the NH_3 synthesis rate.

$$r = {P^n}_{N_2} {P^h}_{H_2} {P^a}_{NH_3} \quad (1)$$

Catalyst Characterization

All of the samples used in the NH_3 synthesis test were passivated with CO_2 (with >99.95% purity, including O_2 as an impurity) and subsequently used for characterization.

High-angle annular dark-field scanning transmission electron microscopy (HAADF-STEM) images and energy dispersive X-ray (EDX) elemental maps were obtained by using a JEM-ARM200CF electron microscope (JEOL, Japan) operated at 120 kV. The samples were dispersed in ethanol at room temperature, dropped on a carbon-coated copper grid, and vacuum dried for 24 h at room temperature.

X-ray diffraction (XRD) analysis was performed by using a SmartLab X-ray diffractometer (Rigaku, Japan) equipped with a Cu Kα radiation source. XRD patterns were analyzed with the PDXL2 software (Rigaku) and three databases (ICDD [18], COD [18], and AtomWork [19]).

The specific surface area of the catalyst after N_2 treatment at 300 °C was measured with a BELSORP-mini apparatus (Bell Japan Corporation, Japan) based on the Brunauer–Emmett–Teller method.

CO chemisorption capacity was measured with a BEL-CAT-II instrument (Micro-Trac BEL, Japan) and used to estimate the turnover frequency of Fe/K(3)/MgO and Fe/MgO. A sample of catalyst (50 mg) was treated with a H_2-N_2 mixture (H_2/N_2 = 3, total 120 mL min^{-1}), and the temperature of the catalyst bed was raised from room temperature to 400 or 500 °C at 2 °C min^{-1}. The sample was held at the same temperature under the H_2-N_2 mixture gas stream for 12 h, purged with a stream of He for 2 h, cooled to 50 °C, and flushed with He for 10 min. After this pretreatment, CO chemisorption analysis was performed at 50 °C in a He flow (30 mL min^{-1}) by pulsed chemisorption.

X-ray fluorescence analysis was performed with an EDXL 300 instrument (Rigaku).

A temperature-programmed reduction (TPR) measurement was performed with a BEL-CAT-II instrument under a flow of 100% H_2 to investigate the reduction behavior of the Fe/K(3)/MgO and Fe/MgO catalysts. For fresh catalyst (before reduction), 50 mg of catalyst was loaded into the reactor, and the temperature was raised from room temperature to 1000 °C at a rate of 10 °C min^{-1}. For catalyst reduction, 50 mg of catalyst sample was treated with a H_2-N_2 mixture (H_2/N_2 = 3, total 120 mL min^{-1}), and the temperature of the catalyst bed was raised from room temperature to 400 or 500 °C at 2 °C min^{-1}. The sample was held at the same temperature in the H_2-N_2 mixture gas stream for 12 h, then cooled to 50 °C and flushed with Ar for 10 min. After this pre-treatment and stabilization of the detector (quadrupole mass spectrometer, BEL-MS, Micro-Trac BEL), the temperature was increased using the same procedure used for fresh catalyst.

Results and Discussion

Ammonia Synthesis Activity of Fe/K/MgO

First, we investigated the NH_3 synthesis activity of Fe/K(3)/MgO. Figure 1 shows the temperature dependence of the NH_3 synthesis rates of Fe/K(3)/MgO, Fe/MgO, and a commercial wüstite-based fused iron catalyst (AmoMax 10RS, Clariant, Japan). The NH_3 synthesis rate of Fe/K(3)/MgO was higher than that of both Fe/MgO and the commercial fused iron catalyst over the investigated temperature range (200–400 °C). At 350 °C, the NH_3 synthesis rate of Fe/K(3)/MgO (17.5 mmol h^{-1} g_{cat}^{-1}) was about 6.6 times higher than that of Fe/MgO and 2.0 times higher than that of the commercial fused iron catalyst (Table 1). The Fe/K(3)/MgO catalyst with Fe nanoparticles effectively catalyzed NH_3 synthesis and exhibited considerable ammonia synthesis activity per Fe unit weight, about 9.1 times higher than the commercial fused iron catalyst containing a bulk form of iron (Table S1). [20]

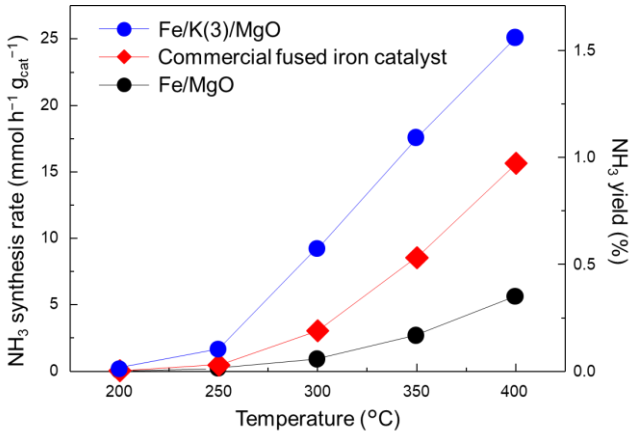

Figure 1. Temperature dependence of NH_3 synthesis rate and yield for Fe/K(3)/MgO, Fe/MgO, and commercial fused iron catalyst at 1.0 MPa.

Next, we investigated the effects of K doping on the catalysts. The rate of NH_3 synthesis was found to differ depending on the doping amount (Figure S1). Fe/K(3)/MgO and Fe/K(5)/MgO catalysts showed similar NH_3 synthesis rates, and their activities were higher than those of Fe/MgO and the other Fe/K/MgO catalysts, suggesting that the optimal amount of K is in the range of 3%–5%. To clarify the final composition of the catalyst, catalyst samples after the NH_3 synthesis test were examined by X-ray fluorescence analysis (Table S2). Decreases in the actual amount of K from the theoretical amount were considered to be due to partial volatilization of K during calcination and reduction because the heat treatment was above the melting point of the K species (e.g., the melting point of KOH is 360 °C). The decrease in the actual amount of Fe from the theoretical amount was considered to be due to partial sublimation of $Fe(acac)_3$ during the heat treatment under the Ar stream. The XRD patterns of these catalysts revealed that the intensity of the peak attributed to the (110) plane of Fe^0 with a body-centered cubic structure (2θ = 44.67°) differed depending on the doping amount of K (Figure S2a). Although the

pattern for the Fe/K(1)/MgO catalyst did not show the Fe^0 peak, that peak was observed in the patterns for the K-free (Fe/MgO) and Fe/K(3, 5, 7)/MgO catalysts, suggesting that the surface structure of the catalysts differed between the K-free and K-doped catalysts. Indeed, the specific surface area of the Fe/K(1)/MgO catalyst was higher than that of the K-free catalyst (Table S2). The Fe^0 peak became sharper with increasing K content (Figure S2b), indicating that increasing the K content resulted in sintering of the Fe^0 nanoparticles. The specific surface area also decreased with increasing K content. The K doping effect and the size of the Fe^0 nanoparticles were in a trade-off relationship, resulting in the maximum NH_3 synthesis activity being afforded by the Fe/K(3)/MgO and Fe/K(5)/MgO catalysts.

Table 1. Physicochemical Properties and Catalytic Performance of Supported Fe Catalysts.

Entry	Catalyst	SSA[a] [$m^2\ g_{cat}^{-1}$]	CO-chemisorption[b] [$\mu mol\ g_{cat}^{-1}$]	Rate[c] [$mmol\ h^{-1}\ g_{cat}^{-1}$]	TOF[d] [s^{-1}]
1	Fe/K(3)/MgO	115	49.5	17.5	0.098
2	Fe/MgO	123	17.0	2.7	0.043
3	Commercial fused iron catalyst	-	-	8.6	-

[a] Specific surface area. [b] Measured as CO-chemisorption capacity. [c] NH_3 synthesis rate at 350 °C and 1.0 MPa. [d] Turnover frequency calculated from the CO-chemisorption value and NH_3 synthesis rate.

.

Next, the effect of pre-reduction temperature on Fe/K(3)/MgO was investigated by pre-reducing at the usual temperatures of 400 and 500 °C as well as at 700 °C, following our previous report on Co@BaO/MgO. [9] Co@BaO/MgO formed a Co-core and BaO-shell structure when pre-reduced at 700°C, a higher temperature than usual, resulting in very high NH_3 synthesis activity under mild conditions. In case of Fe/K(3)/MgO, the highest NH_3 synthesis rate was obtained when the catalyst was pre-reduced at 500 °C (Figure S3). The XRD patterns of these catalysts revealed that the intensity of the Fe^0 peak differed depending on the pre-reduction temperature (Figure S4). The Fe^0 peak became sharper with increasing pre-reduction temperature, indicating that increasing the catalyst pre-reduction temperature resulted in sintering of the Fe^0 nanoparticles. The K/Fe ratio indicated that the high temperature treatment at 700 °C promoted sublimation of K (Table S2). These factors are considered to lower the activity of the catalyst pre-reduced at 700 °C. To determine why the pre-reduced catalyst at 500 °C (Fe^0 peak was detected) showed higher activity than that pre-reduced at 400 °C (Fe^0 peak was not detected), the CO-chemisorption capacity (an index of Fe dispersion) of Fe/K(3)/MgO treated at each reduction temperature was measured (Table S2). The CO-chemisorption capacity was larger for the catalyst pre-reduced at 500 °C than for that pre-reduced at 400 °C, and the ratio of Fe^0 on the surface was larger over the former than the latter catalyst.

To investigate the reduction behavior of Fe/K(3)/MgO, H_2-TPR measurement was performed. We observed three water formation peaks in the m/z = 18 profile of the fresh, non-reduced catalyst, which were attributed to water adsorbed on the sample (at around 100 °C), reduction of Fe^{3+} to Fe^{2+} (at around 350 °C), and reduction of Fe^{2+} to Fe^0 (at around 500 °C) (Figure S5). No such peaks were observed in the m/z = 18 profiles of the catalysts reduced at 400 or 500 °C. In contrast, the m/z = 16 profiles, which were derived from the methanation of residual carbon on the catalyst surface, were different after the pre-reduction at different temperatures. The m/z = 16 profile after pre-reduction at 400 °C showed a methane formation peak above 400 °C, but the profile after pre-reduction at 500 °C showed it above 600 °C. Therefore, because the residual carbon derived from $Fe(acac)_3$ continued to cover part of the Fe surface, the CO-chemisorption capacity was smaller for the catalyst pre-reduced at 400 °C than for that pre-reduced at 500 °C, indicating that the 500 °C pre-reduction was optimum.

Investigation of the effects of different Fe precursors showed that $Fe(acac)_3$ was superior to the more typically used Fe precursor iron (III) nitrate nonahydrate in terms of NH_3 synthesis activity (Figure S6). The lower activity was attributed to the aqueous acid solution (pH = 2.2) used during Fe impregnation, which can damage the basic MgO carrier and greatly decrease the specific surface area and enhance sintering of Fe (Table S2, Figure S7). [21]

Figure 2 shows the pressure dependence of the NH_3 synthesis rate at 350 °C for Fe/K(3)/MgO, Fe/MgO, and two previously reported benchmark Ru catalysts, Cs^+/Ru/MgO and Ru/CeO_2. Cs^+/Ru/MgO is a well-known active Ru catalyst, and Ru/CeO_2 is a good candidate for NH_3 synthesis using renewable energy. [13-14] The NH_3 synthesis rate of Fe/K(3)/MgO was lower than those of the benchmark Ru catalysts at 0.1 MPa but increased drastically with increasing reaction pressure, whereas the rates of the benchmark Ru catalysts did not increase as much. As a result, the NH_3 synthesis rate of Fe/K(3)/MgO was much higher than that of the Ru catalysts at 3.0 MPa. The NH_3 synthesis rate of Fe/MgO was much lower than that of the other catalysts over the investigated pressure range (0.1–3.0 MPa).

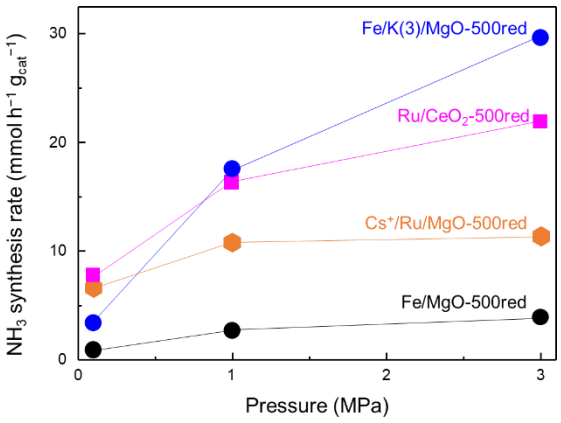

Figure 2. Pressure dependence of the NH_3 synthesis rate of Fe/K(3)/MgO, Fe/MgO, and two benchmark Ru catalysts at 350 °C. xxxred stands for pre-reduction of the catalyst at xxx °C.

We also investigated the stability of Fe/K(3)/MgO and found that NH_3 can be synthesized steadily at the same initial rate at 350 °C and 1.0 MPa for at least 100 h (Figure 3). We also compared the NH_3 synthesis activity of Fe/K(3)/MgO with that of previously reported bulk-type fused Fe catalysts and Fe-based nanoparticle catalysts (Table S3). When the weight hourly space velocity was decreased from 72,000 to 36,000 mL h^{-1} g_{cat}^{-1} for Fe/K(3)/MgO, the NH_3 synthesis rate was 10.4 mmol h^{-1} g_{cat}^{-1} at 350 °C and 1.0 MPa. Fe/K(3)/MgO prepared by a simple impregnation method showed comparable or better activity for NH_3 synthesis than the previously reported Fe-based catalysts under mild conditions.

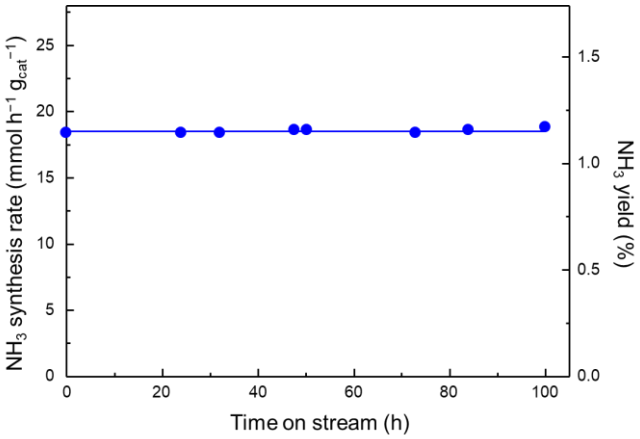

Figure 3. Time course of ammonia synthesis rate over Fe/K(3)/MgO at 350 °C and 1.0 MPa.

Influence of K Doping on the Kinetics of Fe/MgO Catalysts

Next, a kinetic analysis was conducted to evaluate the reasons for the NH_3 synthesis rate dependence on reaction temperature and pressure. Figure 4 shows Arrhenius plots for Fe/K(3)/MgO, Fe/MgO, and a commercial fused iron catalyst. The slope of the plot for Fe/K(3)/MgO changed markedly at 300 °C. For the lower temperature range (200–300 °C, dashed line), the apparent activation energy for Fe/K(3)/MgO, Fe/MgO, and the commercial fused iron catalyst was 96.5, 85.5, and 72.9 kJ mol^{-1}, respectively, indicating that Fe/K(3)/MgO had the highest apparent activation energy. However, for the higher temperature range (300–400 °C, solid line), the apparent activation energy was 32.3, 52.5, and 59.7 kJ mol^{-1}, respectively, indicating that Fe/K(3)/MgO had the lowest apparent activation energy. This suggests that the addition of K to Fe/MgO significantly lowers the apparent activation energy at temperatures of 300 °C and above.

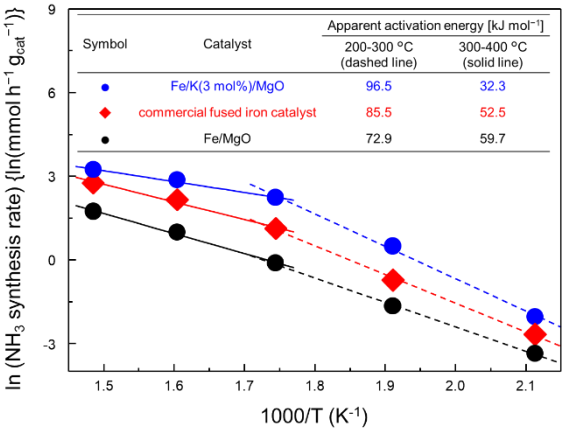

Figure 4. Arrhenius plots for NH_3 synthesis reactions of Fe/K(3)/MgO, Fe/MgO, and a commercial fused iron catalyst at 1.0 MPa.

In the present experiments, measurements were performed in a stepwise manner as the temperature was increased from 200 to 400 °C. Therefore, to examine whether the apparent activation energy of 32.3 kJ mol^{-1} can be retained at a low reaction temperature (<300 °C) after the catalyst had been taken above 300 °C, the NH_3 synthesis test was conducted for a second cycle. After the first cycle, the reactor temperature was kept at 400 °C and 1 MPa for at least 15 h, then the temperature was lowered to 200 °C, and the NH_3 synthesis test was conducted for a second cycle once the NH_3 synthesis rate had become constant. The apparent activation energy for the temperature range of 200–300 °C was 89.7 kJ mol^{-1}, which was slightly lower than the 96.5 kJ mol^{-1} obtained during the first cycle at the same temperature range, but much higher than the 32.3 kJ mol^{-1} obtained at the higher temperature range (Figure S8). Together, these results indicated that the catalytic behavior of Fe/K(3)/MgO was improved during reaction at high temperature (300–400 °C) and that the effect of K doping was obvious at temperatures above 300 °C. In other words, to develop Fe-based catalysts with high NH_3 synthesis activity below 300 °C, it will be necessary to employ a different strategy using elements other than K.

We estimated the N_2, H_2, and NH_3 reaction orders by measuring the influence of N_2, H_2, and NH_3 partial pressure on the NH_3

synthesis rate at 350 °C and 0.1 MPa (Figure S9). The determined reaction orders are summarized in Table 2. The reaction order was investigated with respect to N_2. The reaction orders for the Fe- and Ru-based catalysts were almost at unity, indicating that dissociation of molecular N_2 is the rate-limiting step. In contrast, the reaction order with respect to H_2 differed markedly for the Ru- and Fe-based catalysts: the reaction order with respect to H_2 for Cs^+/Ru/MgO and Ru/CeO_2 was negative, indicating that H atoms are strongly adsorbed on the Ru surface resulting in hydrogen poisoning, which is a typical drawback of Ru catalysts, whereas it was positive for Fe/K(3)/MgO and Fe/MgO. The reaction order with respect to NH_3 was negative for both Ru- and Fe-based catalysts, but both Fe-based catalysts showed large negative values below −1.0, indicating that the NH_x species generated on the Fe surface were strongly adsorbed and that the equilibrium between the NH_x species and molecular NH_3 inhibited the adsorption and activation of N_2.

To further understand the kinetics of the catalysts, the retardation index was considered. [22] Based on the idea that the rate-limiting step is the dissociative adsorption of dinitrogen, this step is retarded by adsorbed species such as NH_x(a) (x = 0, 1, 2) and H(a), and these adsorbed species are in equilibrium with gaseous NH_3 and H_2. Assuming the Langmuir-type rate equation used for Fe catalysts, the rate is given by Eq. 2 below. [23] When the retardation index is described as y for NH_x(a) and z for H(a), the NH_3 synthesis rate can be described as following a power rate form (Eq. 3), which is transformed from Eq. 2:

$$r = k\mathrm{P}_{\mathrm{N}_2}\left(1 + K_1\mathrm{P}_{\mathrm{NH}_3}\mathrm{P}_{\mathrm{H}_2}{}^{-(1.5-0.5x)} + K_2\mathrm{P}_{\mathrm{H}_2}{}^{0.5}\right)^{-2} \quad (2)$$

$$\begin{aligned} r &= k\mathrm{P}_{\mathrm{N}_2}\left(K_1\mathrm{P}_{\mathrm{NH}_3}\mathrm{P}_{\mathrm{H}_2}{}^{-(1.5-0.5x)}\right)^{-2y}\left(K_2\mathrm{P}_{\mathrm{H}_2}{}^{0.5}\right)^{-2z} \\ r &= kK_1{}^{-2y}K_2{}^{-2z}\mathrm{P}_{\mathrm{N}_2}\mathrm{P}_{\mathrm{H}_2}{}^{(3-x)y-z}\mathrm{P}_{\mathrm{NH}_3}{}^{-2y} \\ &= k'\mathrm{P}_{\mathrm{N}_2}\mathrm{P}_{\mathrm{H}_2}{}^{(3-x)y-z}\mathrm{P}_{\mathrm{NH}_3}{}^{-2y} \quad (3) \\ &\quad (k' = kK_1{}^{-2y}K_2{}^{-2z}) \end{aligned}$$

where k is the rate constant for dinitrogen adsorption (Eq. 4), K_1 is the equilibrium constant for NH_3 adsorption (Eq. 5), and K_2 is the equilibrium constant for H_2 adsorption (Eq. 6).

$$\mathrm{N}_2(\mathrm{g}) + 2 * = 2\mathrm{N}(\mathrm{a}) \quad (4)$$

$$\mathrm{NH}_3(\mathrm{g}) + * = \mathrm{NH}_x(\mathrm{a}) + (1.5 - 0.5x)\mathrm{H}_2(\mathrm{g}) \quad (5)$$

$$\mathrm{H}_2(\mathrm{g}) + 2 * = 2\mathrm{H}(\mathrm{a}) \quad (6)$$

(∗: vacant site for adsorption)

By comparing Eqs. 1 and 3, y and z can be calculated using $h = (3 - x)y - z$ and $a = -2y$. The retardation index of Fe/K(3)/MgO was (y, z) = (0.76, −0.01) at 350 °C when x = 0 (Table 3). The value of x is considered to be 0 because $0 < y + z < 1$. This means that the surface of Fe/K(3)/MgO is covered with N(a), and the equilibrium of N(a) + 1.5H_2(g) = NH_3(a) controls the reaction. [24] In contrast, the retardation index of Fe/MgO was (y, z) = (0.68, 0.56) at 350 °C when x = 0, which is not reliable because $y + z > 1$. When x = 1, (y, z) = (0.68, −0.11), which satisfies $0 < y + z < 1$, so the value of x is considered to be 1. This means that the surface of Fe/MgO is covered with NH(a), and the equilibrium of NH(a) + 1.0H_2(g) = NH_3(a) controls the reaction. Thus, K changed the main adsorbed species from NH(a) to N(a), and the activity of Fe/K(3)/MgO increased with increasing pressure, whereas the activity of Fe/MgO did not increase as much owing to the retardation effect of the strongly adsorbed NH species (Figure 2). Therefore, kinetic analysis indicated that the obtained advantage of K doping is not only electron-donation to Fe^0 and structural modification of active sites, which are long-accepted mechanisms, [15-16, 25] but also is the acceleration of the nitrogen dissociation by main adsorption of N(a) species instead of NH(a) on the surface. While non-existence of K atoms in the catalyst structure leads to the retardation of nitrogen dissociation by main adsorption of NH(a) species.

Table 2. Results of kinetic analyses for Fe/K(3)/MgO, Fe/MgO, and two previously reported Ru catalysts.

Catalyst	Analyses Temp. [°C]	Order[a]			Reference
		n	*h*	*a*	
Fe/K(3)/MgO	350	1.00	2.30	−1.53	This work
Fe/MgO		1.16	1.47	−1.35	
Cs^+/Ru/MgO		1.07	−0.76	−0.15	9
Ru/CeO_2		0.85	−0.18	−0.19	
Fe/K(3)/MgO	300	0.87	1.26	−1.03	This work

[a] n, h, and a are the reaction order for N_2, H_2, and NH_3, respectively.

Table 3. Results of kinetic analyses for Fe/K(3)/MgO, Fe/MgO, and two previously reported Ru cat.

Catalyst	Analyses Temp. [°C]	Order[a]		Retardation indexes[b]		
		h	*a*	$y = -0.5a$	$z = (3-x)y-h$	
					$x = 0$	$x = 1$
Fe/K(3)/MgO	350	2.30	−1.53	0.77	−0.01	-
Fe/MgO		1.47	−1.35	0.68	0.56	−0.11
Fe/K(3)/MgO	300	1.26	−1.03	0.52	0.29	-

[a] *h* and *a* are the reaction order for H_2 and NH_3, respectively. [b] *y* and *z* are the retardation index for NH_x(a) and H(a), respectively. If the sum of *y* and *z* exceeds 1 when $x = 0$, then $x = 0$ is not suitable and $x = 1$ or 2 is considered.

To examine why the slope of the Arrhenius plot of Fe/K(3)/MgO in Figure 4 changed markedly at around 300 °C, a kinetic analysis at 300 °C and 0.1 MPa was performed (Figure S9). The reaction order with respect to H_2 (+1.26) was much smaller than that at 350 °C (Table 2). The retardation index was (*y*, *z*) = (0.52, 0.29) at 300 °C when $x = 0$ (Table 3). This means that with increasing temperature, dissociative adsorption of nitrogen is accelerated due to lower hydrogen adsorption (*z* retardation index decreases) and consequently NH_3 synthesis activity improves. But this retardation becomes slightly larger due to absorbed nitrogen species (*y* retardation index increases), resulting in a linear activity behavior with a slight improvement at high temperatures (Figure 1). Due to this phenomenon, the slope of the Arrhenius plot of Fe/K(3)/MgO differs greatly around 300 °C.

Influence of K on the Structure and Catalytic Properties

First, the physicochemical properties of Fe/MgO catalyst were compared with and without K doping (Table 1). The specific surface area of Fe/K(3)/MgO (Entry 1) was smaller than that of Fe/MgO (Entry 2). In contrast, the CO-chemisorption capacity and the turnover frequency of Fe/K(3)/MgO was about 2.9 and 2.3 times higher than that of Fe/MgO, respectively. These results indicate that K has structural and chemical interactions with Fe nanoparticles, resulting in the formation of highly dispersed Fe^0 active sites.

Next, we investigated the surface morphology of Fe/K(3)/MgO and Fe/MgO by STEM observation and elemental distribution mapping (Figures 5 and 6). High-magnification HAADF-STEM images with atomic resolution showed that the contours of the Fe^0 particles were ambiguous due to oxidation in the atmosphere. This made it difficult to calculate a clear particle size distribution. In fact, when the XRD patterns of the samples were measured at about one month after the NH_3 synthesis test, the Fe^0 peak (44.67°) had disappeared (Figure S10). Commercial fused iron catalyst is often treated in air to stabilize the catalyst surface. However, in the MgO-supported Fe catalyst, Fe nanoparticles are considered to be completed oxidation due to its small particle size even after surface passivation treatment. The implication here is that MgO-supported Fe catalysts should be kept without exposure to air after being subjected to NH_3 synthesis testing. EDX elemental maps of Fe/K(3)/MgO collected after the ammonia synthesis test showed that K was localized around the Fe particles (Figure 5b, c, d). This result is in agreement with previous results for K-doped Fe catalysts. [8, 10] On the other hand, EDX elemental mapping for fresh Fe/K(3)/MgO before reduction showed that Fe and K were dispersed over the MgO (Figure S11). These results showed that Fe and K move across the MgO surface during reduction and NH_3 synthesis and that K is enriched in the vicinity of the Fe nanoparticles. EDX elemental maps of Fe/MgO collected after the ammonia synthesis test showed Fe particles as well as some distribution of Fe along the contours of MgO, which was not observed in the EDX elemental map of Fe/K(3)/MgO (Figure 6b, c, d).

To confirm whether Fe is solidly dissolved in MgO, XRD patterns of Fe/K(3)/MgO and Fe/MgO after the ammonia synthesis test were measured (Figure S12). However, since there was no peak shift of MgO to the lower angles (Figure S12), it cannot be concluded from the XRD patterns that Fe was solidly dissolved in the MgO structure. Considering the results of the H_2-TPR analysis, which showed that during pre-reduction at 500 °C most of the Fe is reduced (Figure S13), the Fe that remained on the MgO contour was re-oxidized Fe that had collected at the MgO contours rather than close to unreduced Fe-oxidized species. Because of the morphology change of Fe nanoparticles caused by exposure to air following passivation treatment, the Fe dispersion estimated from the STEM images is not consistent with that estimated from the CO-chemisorption. Considering the effect of re-oxidation, CO-chemisorption is more reliable for estimating the number of Fe atoms available on the surface.

In summary, K moves across the MgO surface during reduction and NH_3 synthesis to reduce the surface energy [9] of Fe nanoparticles and is enriched in the vicinity of the Fe nanoparticles. Appropriate amounts of added K have a structural effect on the dispersion of Fe in Fe/K(3)/MgO, resulting in high CO-chemisorption capacity and turnover frequency.

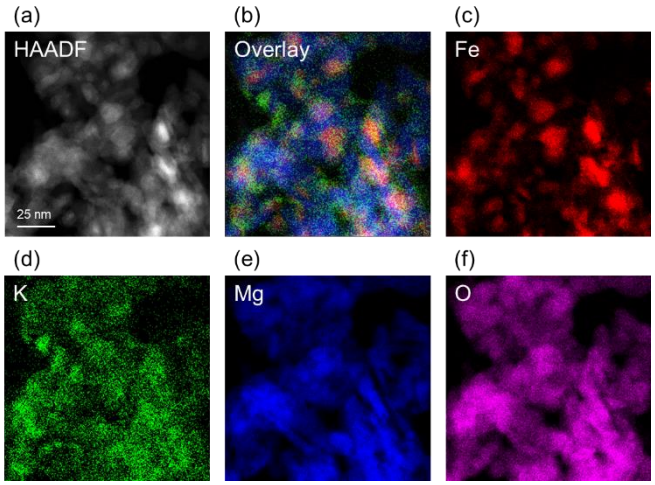

Figure 5. High-angle annular dark-field scanning transmission electron microscopy (HAADF-STEM) images and energy dispersive X-ray (EDX) maps of Fe/K(3)/MgO after ammonia synthesis test. (a) HAADF-STEM image. (b) Overlay EDX maps of Fe K, K K, and Mg K. EDX maps of (c) Fe K, (d) K K, (e) Mg K, and (f) O K. The area in (b–f) is the same as that in (a).

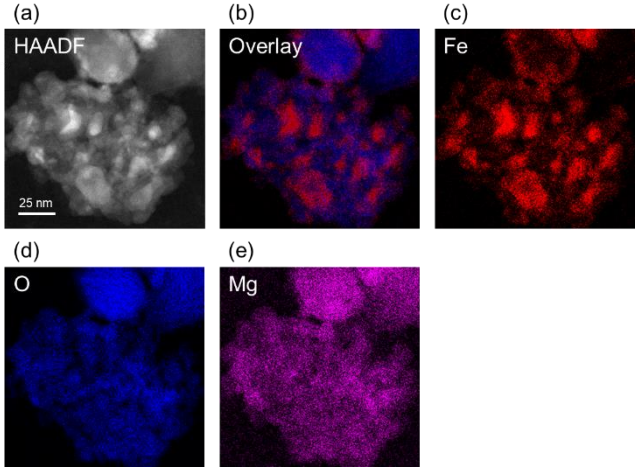

Figure 6. High-angle annular dark-field scanning transmission electron microscopy (HAADF-STEM) images and energy dispersive X-ray (EDX) maps of Fe/MgO after the ammonia synthesis test. (a) HAADF-STEM image. (b) Overlay EDX map of Fe K and Mg K. EDX maps of (c) Fe K, (d) Mg K, and (e) O K. The area in (b–e) is the same as that in (a).

Conclusion

Here, we reported the catalytic behavior of Fe/K(3)/MgO obtained by impregnating iron (III) acetylacetonate into K-doped MgO under mild conditions. At 350 °C and 1.0 MPa, the activity of the Fe/K(3)/MgO catalyst per Fe mass was about 9.1 times higher than that of a commercial fused iron catalyst. Appropriate amounts of K doping increased the dispersion and turnover frequency of Fe in the Fe/K(3)/MgO catalyst. The activity of the catalyst increased with increasing reaction pressure up to 3.0 MPa at the same temperature and was much higher than those of two benchmark Ru catalysts. This is because the Fe/K(3)/MgO catalyst was free from hydrogen poisoning, which is a typical drawback of Ru catalysts. We found that K doping dramatically increased the catalyst's NH_3 synthesis activity, not only because of electron-donation to Fe^0 and structural modification of active sites, which are recognized mechanisms, but also because of accelerating the cleavage of N_2 triple bond by replacing adsorbed NH to N species. The effects of K doping became most evident at temperatures above 300 °C. Morphological observation of the catalyst revealed that K moves across the MgO surface during reduction and NH_3 synthesis and is enriched in the vicinity of Fe nanoparticles. The simple preparation method of Fe/K(3)/MgO used in the present study will facilitate future research into the effects of doping with various elements and/or bimetallization of the catalysts for further enhancement of NH_3 synthesis activity. Our findings show the high potential of Fe nanoparticles for NH_3 synthesis under mild conditions. Such an inexpensive catalyst that exhibits high activity under mild conditions will be an important step for the realization of a green NH_3 synthesis process.

Acknowledgements

Part of the results presented in this article was obtained based on a project (JPNP21012) commissioned by the New Energy and Industrial Technology Development Organization (NEDO). STEM-EDX observations were supported by the "Advanced Research Infrastructure for Materials and Nanotechnology in Japan (ARIM)" of the Ministry of Education, Culture, Sports, Science and Technology (MEXT) (Proposal Number JPMXP1223KU0012). We gratefully acknowledge the financial support from JST FOREST (JPMJFR223N).

Keywords: green ammonia • sustainable energy • energy carrier • Fe nanoparticles • earth-abundant elements

[1] aJ. W. Erisman, M. A. Sutton, J. Galloway, Z. Klimont, W. Winiwarter, *Nat. Geosci.* **2008**, *1*, 636-639; bThe Royal Society, "Ammonia: zero-carbon fertiliser, fuel and energy store", can be found under https://royalsociety.org/topics-policy/projects/low-carbon-energy-programme/green-ammonia/, 2020 (accessed 29 June 2023)

[2] aS. Giddey, S. P. S. Badwal, C. Munnings, M. Dolan, *ACS Sustainable Chem. Eng.* **2017**, *5*, 10231-10239; bA. Valera-Medina, H. Xiao, M. Owen-Jones, W. I. F. David, P. J. Bowen, *Prog. Energy Combust. Sci.* **2018**, *69*, 63-102; cA. Klerke, C. H. Christensen, J. K. Nørskov, T. Vegge, *J. Mater. Chem.* **2008**, *18*, 2304-2310; dK. Eguchi, in *Energy Technology Roadmaps of Japan* (Eds.: Y. Kato, M. Koyama, Y. Fukushima, T. Nakagaki), Springer Japan, **2016**, pp. 167-181; eH. Kobayashi, A. Hayakawa, K. D. K. A. Somarathne, E. C. Okafor, *Proceedings of the Combustion Institute* **2019**, *37*, 109-133; fY. Wang, Y. Tian, S. Y. Pan, S. W. Snyder, *ChemSusChem* **2022**, *15*, e202201290.

[3] S. L. Foster, S. I. P. Bakovic, R. D. Duda, S. Maheshwari, R. D. Milton, S. D. Minteer, M. J. Janik, J. N. Renner, L. F. Greenlee, *Nat. Catal.* **2018**, *1*, 490-500.

[4] A. Mittasch, W. Frankenburg, *Adv. Catal.* **1950**, *2*, 81-104.

[5] K. Sato, K. Nagaoka, *Chem. Lett.* **2021**, *50*, 687-696.

[6] aK. Aika, *Catal. Today* **2017**, *286*, 14-20; bM. Hattori, S. Iijima, T. Nakao, H. Hosono, M. Hara, *Nat. Commun.* **2020**, *11*, 2001; cM. Kitano, Y. Inoue, M. Sasase, K. Kishida, Y. Kobayashi, K. Nishiyama, T. Tada, S. Kawamura, T. Yokoyama, M. Hara, H. Hosono, *Angew. Chem. Int. Ed.* **2018**, *57*, 2648-2652; dK. Sato, S.-i. Miyahara, Y. Ogura, K. Tsujimaru, Y. Wada, T. Toriyama, T. Yamamoto, S. Matsumura, K. Nagaoka, *ACS Sustainable Chem. Eng.* **2020**, *8*, 2726-2734.

[7] P. Wang, F. Chang, W. Gao, J. Guo, G. Wu, T. He, P. Chen, *Nat. Chem.* **2017**, *9*, 64-70.

[8] W. Al Maksoud, R. K. Rai, N. Morlanés, M. Harb, R. Ahmad, S. Ould-Chikh, D. Anjum, M. N. Hedhili, B. E. Al-Sabban, K. Albahily, L. Cavallo, J.-M. Basset, *J. Catal.* **2021**, *394*, 353-365.

[9] K. Sato, S. Miyahara, K. Tsujimaru, Y. Wada, T. Toriyama, T. Yamamoto, S. Matsumura, K. Inazu, H. Mohri, T. Iwasa, T. Taketsugu, K. Nagaoka, *ACS Catal.* **2021**, *11*, 13050-13061.

[10] H. Fan, X. Huang, K. Kahler, J. Folke, F. Girgsdies, D. Teschner, Y. Ding, K. Hermann, R. Schlogl, E. Frei, *Acs Sustainable Chemistry & Engineering* **2017**, *5*, 10900-10909.

[11] P. Q. Yan, W. H. Guo, Z. B. Liang, W. Meng, Z. Yin, S. W. Li, M. Z. Li, M. T. Zhang, J. Yan, D. Q. Xiao, R. Q. Zou, D. Ma, *Nano Res.* **2019**, *12*, 2341-2347.

[12] M. Hattori, N. Okuyama, H. Kurosawa, M. Hara, *J. Am. Chem. Soc.* **2023**, *145*, 7888-7897.

[13] T. Nanba, Y. Nagata, K. Kobayashi, R. Javaid, R. Atsumi, M. Nishi, T. Mochizuki, Y. Manaka, H. Kojima, T. Tsujimura, H. Matsumoto, T. Fujimoto, K. Suzuki, T. Oouchi, S. Kameda, Y. Hoshino, S. Fujimoto, M. Kai, Y. Fujimura, *J. Jpn. Petrol. Inst.* **2021**, *64*, 1-9.

[14] R. Javaid, H. Matsumoto, T. Nanba, *ChemistrySelect* **2019**, *4*, 2218-2224.

[15] G. Ertl, S. B. Lee, M. Weiss, *Surf. Sci.* **1982**, *114*, 527-545.

[16] C. F. Huo, B. S. Wu, P. Gao, Y. Yang, Y. W. Li, H. J. Jiao, *Angew. Chem. Int. Ed.* **2011**, *50*, 7403-7406.

[17] aK. Aika, J. Kubota, Y. Kadowaki, Y. Niwa, Y. Izumi, *Appl. Surf. Sci.* **1997**, *121-122*, 488-491; bR. Kojima, K. Aika, *Applied Catalysis a-General* **2001**, *218*, 121-128; cK. Imamura, S. Miyahara, Y. Kawano, K. Sato, Y. Nakasaka, K. Nagaoka, *J. Taiwan Inst. Chem. Eng.* **2019**, *105*, 50-56.

[18] S. Grazulis, D. Chateigner, R. T. Downs, A. F. Yokochi, M. Quiros, L. Lutterotti, E. Manakova, J. Butkus, P. Moeck, A. Le Bail, *J. Appl. Crystallogr.* **2009**, *42*, 726-729.

[19] Y. Xu, M. Yamazaki, P. Villars, *Jpn. J. Appl. Phys.* **2011**, *50*, 11RH02.

[20] Clariant International Ltd, “Catalysts and Adsorbents for SYNGAS”, can be found under file:///C:/Users/k_jin/Dropbox/PC/Downloads/Clariant%20Brochure%20Catalysts%20And%20Adsorbents%20For%20Syngas%202017%20EN.pdf, 2017 (accessed 29 June 2023)

[21] M. Boudart, A. Delbouille, J. A. Dumesic, S. Khammouma, H. Topsoe, *J. Catal.* **1975**, *37*, 486-502.

[22] K. Aika, M. Kumasaka, T. Oma, O. Kato, H. Matsuda, N. Watanabe, K. Yamazaki, A. Ozaki, T. Onishi, *Appl. Catal.* **1986**, *28*, 57-68.

[23] K. Aika, A. Ozaki, *J. Catal.* **1969**, *13*, 232.

[24] K. Altenburg, H. Bosch, J. G. Vanommen, P. J. Gellings, *J. Catal.* **1980**, *66*, 326-334.

[25] D. R. Strongin, G. A. Somorjai, *J. Catal.* **1988**, *109*, 51-60.

Entry for the Table of Contents

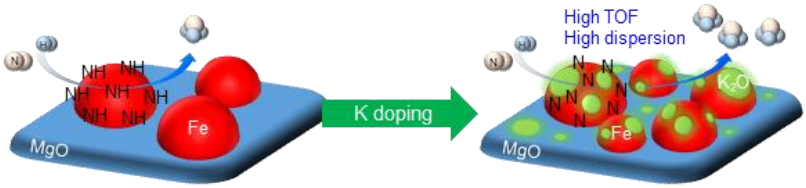

K doping increases the dispersion and turnover frequency (TOF) of Fe and enhances the ammonia synthesis activity at ≥300 °C. This is not only because of electron-donation to Fe^0 and structural modification of active sites, but also because of accelerating the cleavage of N_2 triple bond by replacing adsorbed NH to N species.